

Increasing the effective sampling rate of thermographic imaging for thermal transient analysis

by Simon H. Anke^{*}, Nils J. Ziegeler^{*,**}, Peter W. Nolte^{***}, Stefan Schweizer^{*,***}

^{*} Faculty of Electrical Engineering, South Westphalia University of Applied Sciences, 59494 Soest, Germany

^{**} Thermal and Climate Management, Hella GmbH & Co. KGaA, 59552 Lippstadt, Germany

^{***} Fraunhofer Application Center for Inorganic Phosphors, Branch Lab of Fraunhofer Institute for Microstructure of Materials and Systems IMWS, 59494 Soest, Germany

Abstract

With decreasing electric components sizes, heat management becomes a more challenging part in electronic engineering. In addition, project timelines are compressed, giving less time for multiple loops and iterations. This pressures temperature measurements to be fast, comprehensive, and accurate. With its contactless and spatially-resolved characteristics, thermography is a valuable technique to provide measurements for thermal analysis of complex circuits. Opportunities for optimization are found in providing high temporal and spatial resolution simultaneously. This study presents a sampling technique, so-called super-frequency sampling, that significantly increases the temporal resolution without decreasing spatial resolution for thermal transient analysis. The principle is demonstrated by tests on a high-power LED. The results indicate an increased sampling frequency by almost a factor of ten.

1. Introduction

Thermography serves as a well-established technique for monitoring the temperature of electronic components [1]. As electronic components decrease in size, circuits are being designed in more confined spaces and thermal interaction between the various components becomes more important. These trends challenge existing measurement techniques to provide the information needed to validate detailed computer simulations.

One proven method for characterizing the heat path of an electronic component is thermal transient analysis [2]. The temperature measurements required are typically based on the temperature dependence of certain electrical properties. For instance, the temperature dependence of the forward voltage of a diode can be used to obtain its junction temperature. Thermal transient measurements based on a temperature-sensitive parameter of such a device provides the thermal response of the device at its driving point, i.e. the junction. This response function is known as the thermal impedance. For one-dimensional heat paths, the thermal resistances and capacities along this heat path can be determined using the method of network identification by deconvolution [3].

Temperature measurements on semiconductor components based on temperature-sensitive device parameters are common in thermal transient analysis. Sampling rates typically fall within the megahertz range. As the behavior in the range between 10 μ s and 50 μ s is covered by electrical transients during switching, it must be approximated via extrapolation [4, 5]. Here, thermography has the big advantage that electrical transients do not exist. This allows the use of an infrared detector to its full potential without any component-based limits on sampling rate. In addition, thermal imaging directly captures the temperature distribution of the surface, providing an accurate map of temperature variations across the component under study.

The thermal interaction between electronic components is described by the transfer impedances, which are obtained by heating one component and measuring the response in another. Measuring all desired transfer impedances electrically is challenging in complex circuits due to the accessibility of the components. For each component, a calibration measurement is required to determine the temperature dependence of the electrical property. Furthermore, often additional electrical contacts are needed to connect the individual components to the measuring system. Thermography simplifies this, as it is able to evaluate the thermal interaction between the components contact-free by providing spatially-resolved thermal transients of the entire surface.

While it can take up to several hundreds of seconds for an entire electronic device to reach steady-state conditions, subcomponents have much shorter thermal time constants. Solder point temperatures can respond on time scales of several milliseconds [6]. Electrical measurements can sample these transients at a frequency of one megahertz. Thermography systems usually have a sampling frequency up to a few hundred hertz. Apart from the integration time of the camera itself, the dead time caused by the read-out subsystem is the main limiting factor for the maximum sampling frequency. During the dead time of the detector no signal is recorded. When repeating measurements with a sufficiently accurate relative timing it is possible to place the integration times in sections, where no signal was recorded in previous measurements due to the dead time. In this way, effective sampling rates can be achieved which are much faster than a few hundred hertz at full spatial resolution. One way to conduct repeated thermal transient measurements is to periodically repeat the thermal excitation signal with an appropriate frequency.



In this work, a periodic sampling technique, so-called super-frequency sampling, is demonstrated by tests on a high-power LED. Effectively eliminating the impact of the dead time, an increase in sampling frequency by almost a factor of ten is achieved.

2. Theory

2.1 Thermal transient analysis

Simulations of temperature responses are based on thermal models such as a thermal network composed of thermal resistances. The thermal resistance between two points is given by their temperature difference divided by the heat that flows between them. In analogy to an electrical network, temperature differences correspond to electrical voltages and heat flows to electrical currents. This model enables accurate prediction of component behavior under steady-state conditions [7].

However, to model dynamic behavior, models are expanded by capacitive elements. To analyze these resistance-capacitance networks, the step response of a system is recorded and then converted into the thermal impedance, $Z_{th}(t)$, by

$$Z_{th}(t) = \frac{T(t) - T_0}{\Delta P} \quad (1)$$

with the temperature response on the step excitation, $T(t)$, the steady state temperature before the excitation, T_0 , and the power change at the step, ΔP . From the thermal impedance, the thermal network is derived by calculating the derivative of the thermal impedance, the time constant spectrum, and finally the structure function. The thermal network of electronic components can be extracted from thermographically-measured temperature responses via thermographic network identification [8] or from electrically-measured temperature responses [2].

2.2 Super-frequency sampling

Super-frequency sampling (SFS) is a method to increase the temporal resolution of a periodically-repeated signal. In an SFS measurement scheme, a rectangular excitation signal is applied to the device under test for several periods. The infrared camera records the resulting heating and cooling curves continuously with the camera's sampling frequency not being synchronized to the excitation signal. For appropriate sampling and excitation frequencies, the signal is measured with a slightly increasing offset for each repetition. Subsequently, the obtained time series is collapsed to a single period. For achieving an N -times increase in sampling rate, the signal must be measured at least N times. To collapse all measured periods into a single period, exact knowledge of the period length is required. The signal length observed by the infrared camera is generally slightly different from the excitation frequency, as the sampling and excitation signals are not synchronized. The exact frequency, however, is extracted from the measurement data by the super-frequency sampling algorithm.

2.3 Deterministic Pulse Algorithm

The above-described method of SFS requires relatively long measurement times, as the system needs a relatively long time after each excitation step to return to its steady state. In the case of an LED mounted on an aluminum insulated metal substrate (IMS), the total response takes approximately one hundred seconds. This leads to a relatively long measurement time if several periods are to be recorded using SFS. As suggested by Schmidt *et al.* [9], the total measurement time can be significantly reduced by using incomplete transients and applying an offset-correction to the recorded signal. The focus here is set on short times after a power step, where the impact on an improved temporal resolution is the largest. For the long-time response, there is no need for SFS as thermal dynamics are exponentially slow and conventional sampling is perfectly adequate. This is achieved using an algorithm called the deterministic pulse algorithm.

Figure 1 illustrates the workflow of the deterministic pulse algorithm, which consists of two separate measurements: (i) a full thermal transient analysis (TTA) employing a single step and (ii) a deterministic pulse measurement comprising multiple truncated transient measurements. For full TTA, the system is excited by a step input, which is shown in (a). The measurement is long enough to allow the system to return to its thermal equilibrium again, as shown in (b), before the next power step is applied. Subsequently, the thermal impedance is computed (c), following the definition in Section 2.1.

To enhance the signal-to-noise ratio, the thermal impedance is low-pass filtered using a Savitzky-Golay filter of second order, following the procedure as described by Schmidt *et al.* [9]. The filtering process is applied using all points in a certain logarithmic distance from the target measurement point, as opposed to using a fixed number of points around the measurement point. The filtered impedance serves two primary purposes: First, it provides the later part of the thermal impedance, as illustrated in (d), and it gives a basis to calculate the offsets of the deterministic pulse measurements.

In the deterministic pulse algorithm, multiple step responses are performed, as depicted in (f). To increase the sampling frequency with deterministic pulses, the duration of the pulses must be chosen appropriately. For an N -times increased sampling frequency, the following approach is appropriate to choose the time, $\Delta\tau_{DPA}$, between the deterministic pulses. For a sampling period, Δt_s , given by the thermography camera and the time, $\Delta\tau'_{DPA}$, in which the sampling frequency is to be increased, the time between two pulses has to be chosen by use of Eq. (2). The time $\Delta\tau'_{DPA}$ has to fulfill the additional

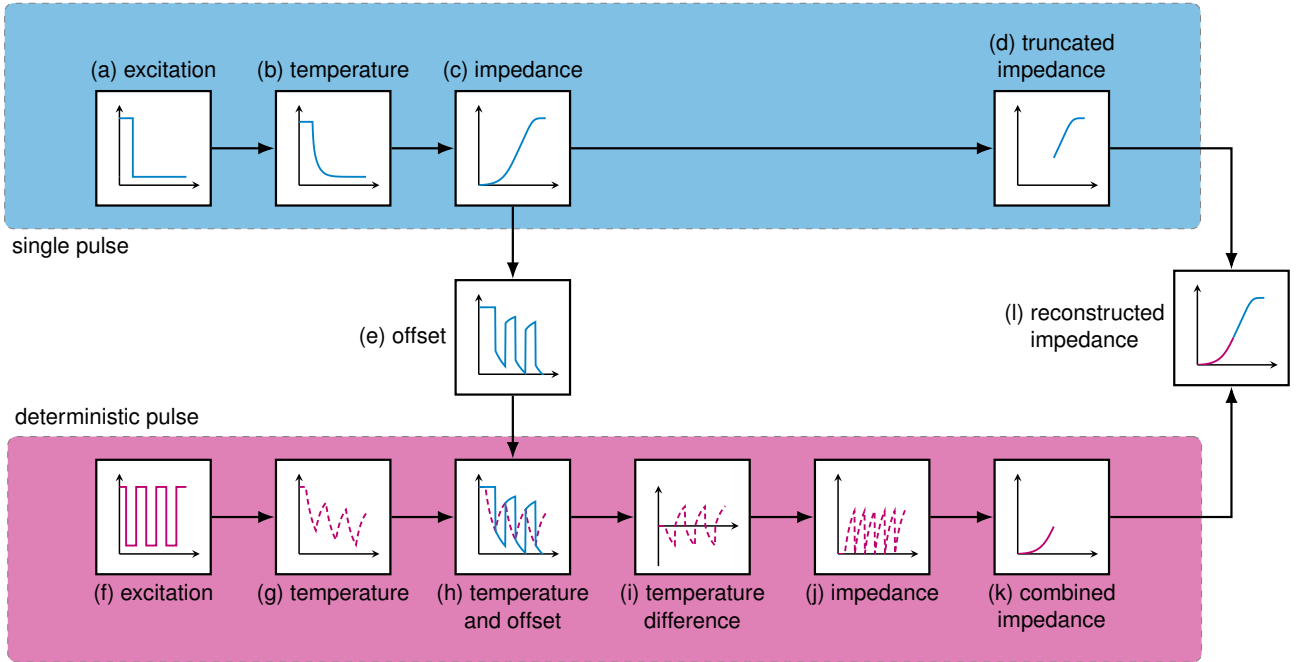


Fig. 1. Flowchart of the deterministic pulse algorithm. It consists of two measurements: in blue the long-term measurement of a full single step response and in pink the measurement of the deterministic pulse response. The full step response is transformed to the thermal impedance and low pass filtered. The filtered impedance is used to calculate the offsets of the deterministic pulse response. After offset correction, the responses of the deterministic pulses are transformed to a thermal impedance and combined to a more densely sampled sequence. Finally, the full and deterministic pulse thermal impedances are combined.

constraint, $\Delta\tau'_{\text{DPA}} \bmod \Delta t_s = 0$.

$$\Delta\tau_{\text{DPA}} = \Delta\tau'_{\text{DPA}} + \frac{\Delta t_s}{N} \quad (2)$$

In the system's responses, as shown in (g), each response is superimposed by all previous responses. To extract the single-step short-time responses, the contribution of the superimposed previous pulses, $\Delta T_{\text{offset}}(t)$, must be subtracted. This offset is shown in (e) and calculated as

$$\Delta T_{\text{offset}}(t) = T_0 + \begin{cases} 0 & \text{if } t < t_{\Delta P,1} \\ \Delta P_0 \cdot Z_{\text{th}}(t - t_{\Delta P,0}) & \text{if } t_{\Delta P,1} \leq t < t_{\Delta P,2} \\ \Delta P_0 \cdot Z_{\text{th}}(t - t_{\Delta P,0}) + \Delta P_1 \cdot Z_{\text{th}}(t - t_{\Delta P,1}) & \text{if } t_{\Delta P,2} \leq t < t_{\Delta P,3} \\ \dots & \dots \\ \sum_{j=0}^{i-1} \Delta P_j \cdot Z_{\text{th}}(t - t_{\Delta P,j}) & \text{if } t_{\Delta P,i+1} \leq t < t_{\Delta P,i+2} \quad \text{for } i = \{0, \dots, M-2\} \\ \sum_{j=0}^{i-1} \Delta P_j \cdot Z_{\text{th}}(t - t_{\Delta P,j}) & \text{if } t_{\Delta P,i+1} \leq t \quad \text{for } i = M-1 \end{cases} \quad (3)$$

with the j -th power change, ΔP_j , at the time, $t_{\Delta P,j}$, the initial temperature, T_0 , the thermal impedance, $Z_{\text{th}}(t)$, and the number of power changes, M . The initial temperature is extracted by the measurement points before a pulse is applied to the system. To improve the accuracy of the offset correction for each step response in the range $(t_{\Delta P,i}, t_{\Delta P,i+1})$, the magnitude of the previous power change, ΔP_i , is optimized to the measured temperature by minimizing the following loss function

$$f(\Delta P_i) = \int_0^{t_{\text{max}}} \left| T(t) - T_0 - \begin{cases} \Delta P_0 \cdot Z_{\text{th}}(t - t_{\Delta P,0}) & \text{if } t < t_{\Delta P,1} \quad \text{for } i = 0 \\ \dots & \dots \\ \sum_{j=0}^i \Delta P_j \cdot Z_{\text{th}}(t - t_{\Delta P,j}) & \text{if } t < t_{\Delta P,i+1} \quad \text{for } i = \{0, \dots, M-2\} \\ \sum_{j=0}^i \Delta P_j \cdot Z_{\text{th}}(t - t_{\Delta P,j}) & \text{for } i = M-1 \end{cases} \right| dt. \quad (4)$$

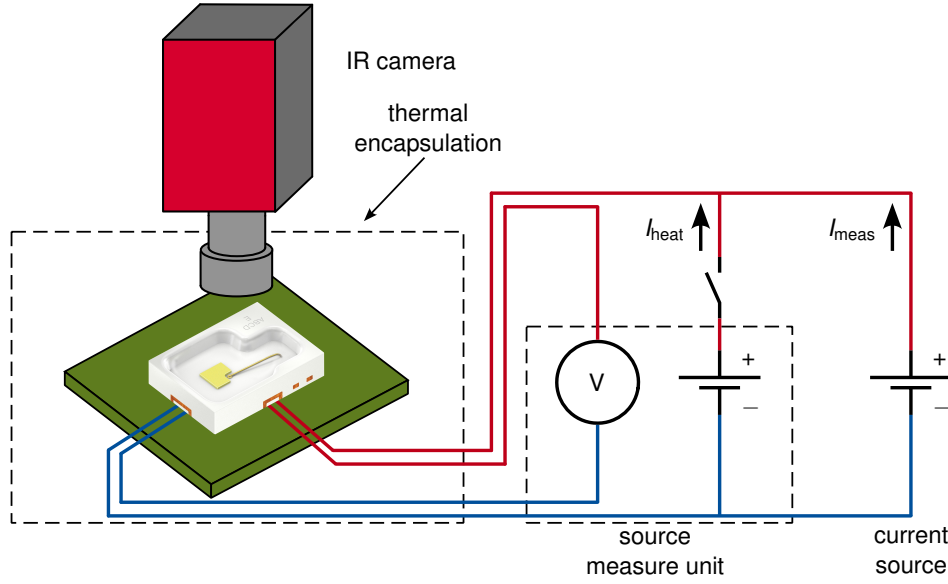


Fig. 2. Scheme of the measurement setup. The LED is placed in a temperature controlled thermal encapsulation. The measuring current, I_{meas} , is supplied by a current source and the heating current, I_{heat} , by a source measure unit. The heating current is switched by a relay. Additionally, the voltage of the LED is measured by the source measure unit. The temperature of the LED is measured with an IR camera with a microscope objective lens. The relay, the source measure unit, and the IR camera are controlled and triggered with a PC.

With the system's response, $T(t)$, and the offset of the previous pulses, $\Delta T_{offset}(t)$, as depicted in (h), the short-time responses are calculated as $\Delta T(t) = T(t) - \Delta T_{offset}(t)$ and shown in (i). The thermal impedance for each pulse is then calculated using the individually adjusted power step for each pulse, as depicted in (j). For the combination of the different impedances, each pulse is shifted to zero as

$$t'_i = \begin{cases} t_i \bmod t_{\Delta P,0} & \text{if } t_{\Delta P,0} \leq t_i < t_{\Delta P,1} \\ \dots & \dots \\ t_i \bmod t_{\Delta P,M-2} & \text{if } t_{\Delta P,M-2} \leq t_i < t_{\Delta P,M-1} \\ t_i \bmod t_{\Delta P,M-1} & \text{if } t_{\Delta P,M-1} \leq t_i \end{cases} \quad (5)$$

The points prior to the first power change are not used for the combination. The combined impedance from the deterministic pulses is shown in (k). For the combination of the full thermal impedance in (d) and the thermal impedance of the deterministic pulse sequence in (k), the transition between the two impedances needs to be smooth.

3. Experimental details

The device under test is a white, surface-mounted device (SMD) LED soldered to an aluminum printed circuit board (PCB). The color-converting element (CCE) consists of a thin layer mounted directly on top of the chip with a fill-in applied to protect both, the chip and the phosphor. The dimensions of the LED are 2.75 mm × 2 mm × 0.6 mm. For a defined environment temperature, the PCB is mounted onto a temperature-controlled aluminum baseplate and placed inside a thermally-insulated box. A thermoelectric cooler (Arroyo Instruments 207 TEC LaserMount) serves as heatsink. For operating the LED, two source measure units are used: the first (Keithley 2400) provides the measuring current, I_{meas} , the second (Keithley 2461) the heating current, I_{heat} . The second measure unit also records the heating current and the voltage at the LED. The heating current is switched on and off with a relay, which is operated by a data acquisition (DAQ) USB device (NI USB-6003). The thermography camera system is an InfraTec ImageIR 8380S (mid-IR). The measurement of the Keithley 2461 and the camera system are synchronized with the DAQ USB device. A scheme of the measurement setup is shown in Figure 2.

The currents applied to the LED are $I_{meas} = 1$ mA and $I_{heat} = 600$ mA. The sampling rate of the thermography camera is set to 200 Hz, that of the DAQ USB device to 2 kHz. As the speed-up factor and the shift of pulses are related to each other according to Eq. (2), the maximum possible speed-up factor is limited by the sampling rate of the DAQ USB device and amounts to $N = \Delta t_s / \Delta t_r = f_r / f_s = 10$. The calculated distance between two cooling pulses amounts to $2\text{ s} + 5 \cdot 10^{-4}\text{ s}$.

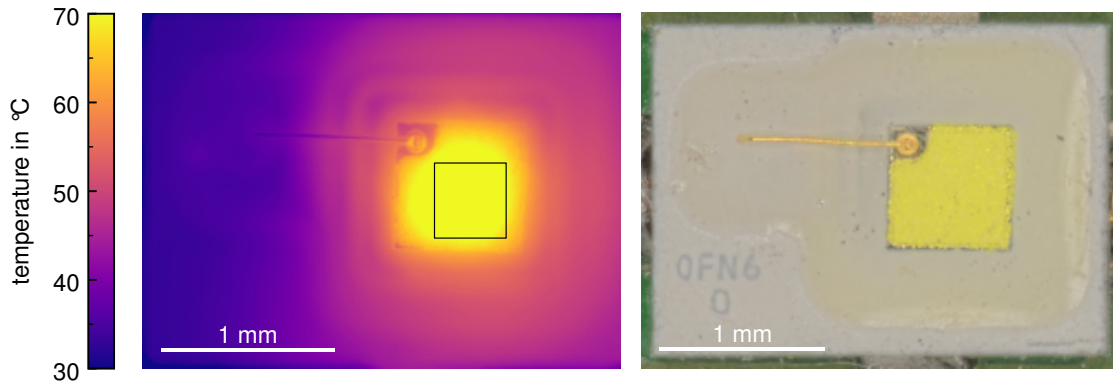


Fig. 3. (left) Thermographic microscopy image with the LED on. (right) Optical microscopy image with the LED off.

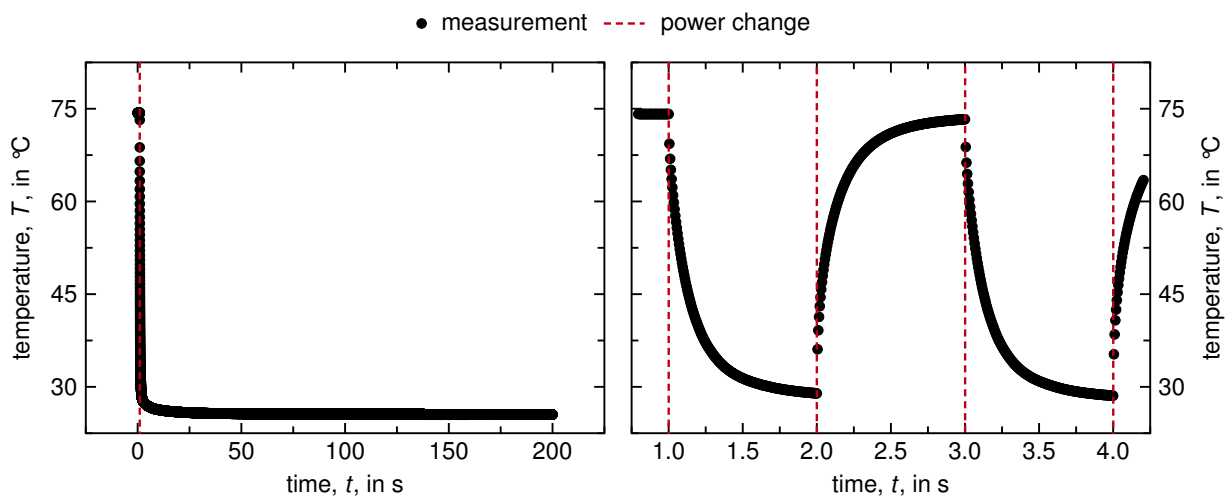


Fig. 4. Temporal behavior of the mean temperature of the test area on the LED chip. (left) Full transient response during cooling, (right) responses to the deterministic pulses. The positions of the power changes are indicated by dashed vertical lines.

4. Results and Discussion

To evaluate the performance of the proposed super-frequency sampling method, thermographic measurements are performed using a range of excitation signals as detailed in Section 2.3. Figure 3 displays a thermographic microscopy image (left) taken at an applied current of 601 mA as well as an optical microscopic image (right) of the LED used in the experiments. The algorithm's evaluation is focused on the mean temperature within a designated 83×87 pixel area on the LED chip, as indicated by a black square in the thermographic image. Figure 4 provides comparative temperature profiles: (left) full transient response during cooling, (right) responses to the deterministic pulses. For clarity, only the first periods of the deterministic pulse measurement are presented. The complete measurement sequence includes ten cooling and ten heating pulses to achieve a tenfold speed-up. In both figures, the positions of the power changes during the measurement process are marked.

The full measurement is transformed to the thermal impedance, as described in Section 2.1, and subsequently filtered with a second-order Savitzky-Golay filter. As the electrical parameters of the LED are temperature-dependent, the voltage across the LED and thus the heating power change accordingly. This results in an excitation curve deviating from a pure rectangular waveform. Given the low current during the cooling phases, the power change during these periods is negligible.

There are two possible approaches to address this issue. The first approach is based on the power profile during the heating phase to apply an offset correction. The second approach, which is applied in this work, involves measuring an additional full single step response for a turn-on power change. The thermal impedance obtained from this measurement is then used to determine the offsets caused by the positive changes in power. For both approaches, the heating phase cannot be used to increase the sampling rate in the case of an LED presented here.

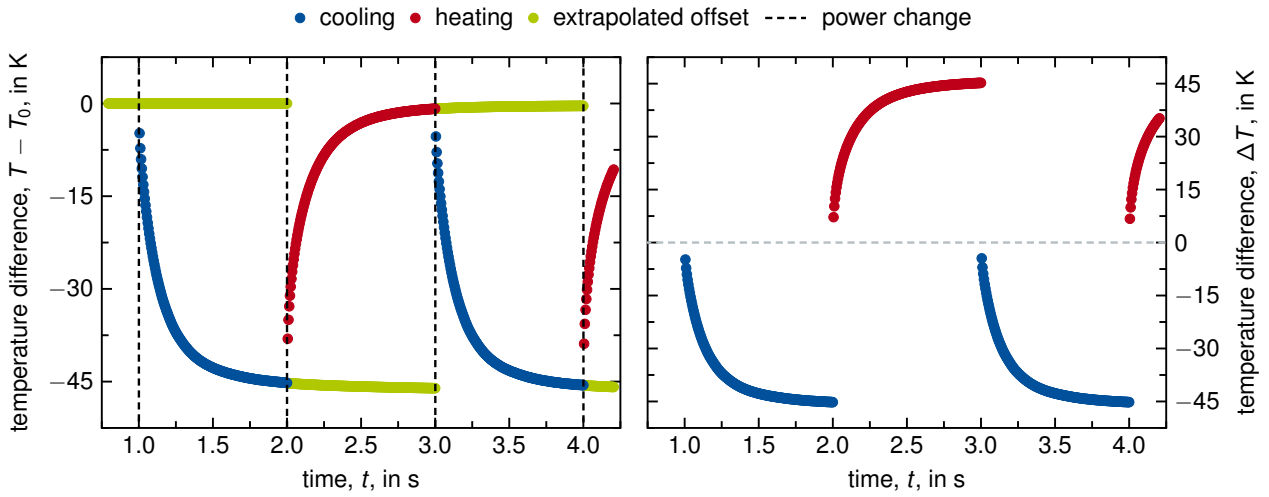


Fig. 5. (left) Deterministic pulse measurement, $T(t)$, and the extrapolated offsets, $\Delta T_{\text{offset}}(t)$, with the initial temperature, T_0 , subtracted. The positions of the power changes are indicated as dashed vertical lines. (right) Resulting offset-corrected short-time responses of the LED, $\Delta T(t)$.

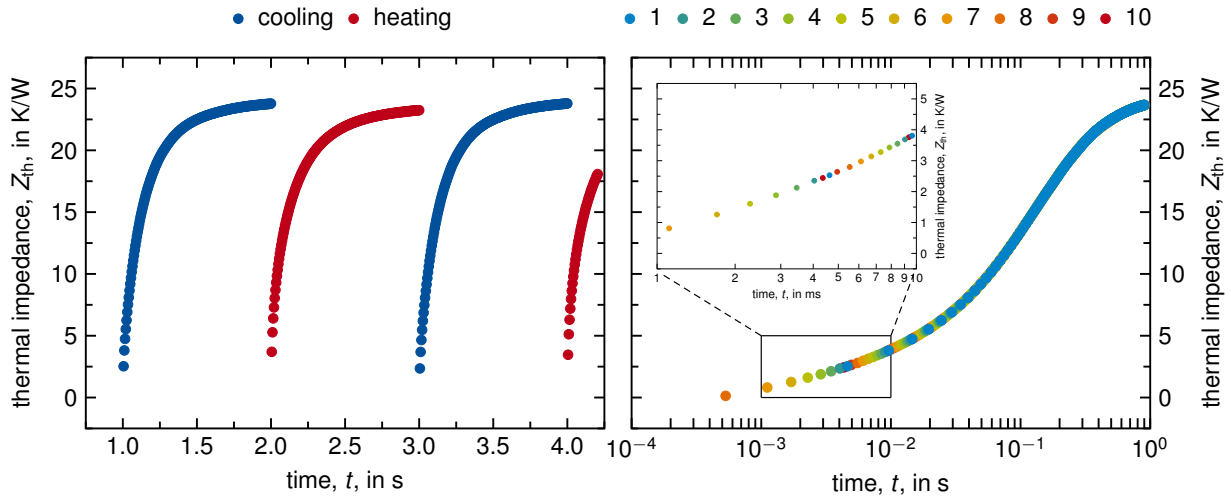


Fig. 6. (left) Thermal impedance for the different pulses. (right) Reconstructed thermal impedance of the cooling transient. The data points are color-coded according to the original transient.

To determine time, $t_{\Delta P}$, and initial magnitude of the power step, ΔP , electrical measurements are used. Both, time and power step, serve as input parameter for the optimization according to Eq. 4. The power is estimated by taking the difference between the power shortly before and after the power step. The power step is considered as finished, after the current has reached steady state again.

For the evaluation of the deterministic pulse measurement, the initial temperature, T_0 , is extracted from the measurement by calculating the mean of the data points prior to the first deterministic pulse. Figure 5 (left) shows the difference between the initial temperature and the measured temperature in the deterministic pulse measurement and its extrapolated offset. The short-time responses are shown in Figure 5 (right). The thermal impedance is obtained by dividing the temperature difference by the corresponding power change, as shown in Figure 6 (left). The non-constant heating power shows up as a difference in the shape of the heating and cooling impedance. In a subsequent step, the impedances are combined, as shown in Figure 6 (right). The points are color-coded according to their original period. The inset shows the range between 1 ms and 10 ms in detail. There, the data points of period 10 are between period 1 and 2. This phenomenon is induced by the DAQ USB device, as the period duration differs from the expected 5 ms, it exceeds this value.

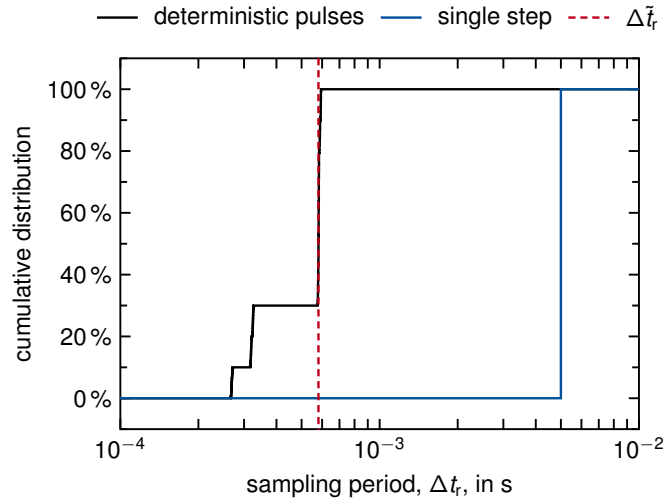


Fig. 7. Cumulative distribution of sampling periods within the reconstructed thermal impedance in the range of $0\text{ s} < t'_i < 1\text{ s}$, its median $\Delta\tilde{t}_r = 5.8 \cdot 10^{-4}\text{ s}$, and the sampling periods within the full cooling impedance with 200 Hz.

To analyze the temporal resolution of the reconstructed signal, the reconstructed sampling period, $\Delta t_{r,i} = t'_{i+1} - t'_i$, is calculated for the data points in the range $0\text{ s} < t'_i < 1\text{ s}$. The cumulative distribution of the reconstructed sampling periods and its median of $5.8 \cdot 10^{-4}\text{ s}$ are shown in Figure 7. The resulting speed-up factor is

$$N_{\Delta t_r} = \frac{\Delta t_s}{\Delta\tilde{t}_r} = \frac{5 \cdot 10^{-3}\text{ s}}{5.8 \cdot 10^{-4}\text{ s}} = 8.6. \quad (6)$$

5. Conclusion

In this study, super-frequency sampling is combined with the method of deterministic pulses, significantly enhancing the temporal resolution of thermographic measurements from 200 Hz to 1.72 kHz. The combination eliminates the dead time limitations of thermography cameras, providing more precise thermal transient analysis at full spatial resolution. The application of deterministic pulses with power optimization demonstrated smoother reconstructions of thermal transients and reduced the impact of temperature drift, resulting in improved accuracy and reliability.

The main steps of the method include applying a particularly chosen periodic excitation signal to the device under test, continuously recording the thermal response with an infrared camera, and combining the measured step responses to construct a single thermal impedance. Deterministic pulses are used to focus on short-time responses. The resulting data is processed to reconstruct high-resolution thermal transients. This process is validated through tests on a high-power LED, demonstrating a tenfold increase in sampling frequency and reduced measurement time.

This advancement holds potential for various fields that require precise thermal management, such as electronics cooling as well as thermal transient analysis. However, challenges remain, in particular for LEDs, as continuous power changes during heating phases limit the precision of the offset correction. To increase the sampling frequency further, higher accuracy of excitation signals and triggings is required.

References

- [1] A. Stoyanova, B. Bonev, N. Kafadarova, and S. Rizanov. Infrared measurements of temperature anomalies in electronic devices. In *2022 IEEE 9th Electronics System-Integration Technology Conference (ESTC)*, pages 509–515, 2022.
- [2] M. Rencz, G. Farkas, and A. Poppe. *Theory and Practice of Thermal Transient Testing of Electronic Components*. Springer Cham, 1st edition, 2023.
- [3] V. Szekely. Identification of rc networks by deconvolution: chances and limits. *IEEE Transactions on Circuits and Systems I: Fundamental Theory and Applications*, 45(3):244–258, 1998.
- [4] JEDEC Solid State Technology Association. JESD51-51: Implementation of the Electrical Test Method for the Measurement of Real Thermal Resistance and Impedance of Light-Emitting Diodes with Exposed Cooling. April 2012.

- [5] CIE International Commission on Illumination. CIE 225: Optical Measurement of High-Power LEDs. 2017.
- [6] A. Griesinger. *Wärmemanagement in der Elektronik: Theorie und Praxis*. Springer Vieweg Berlin, 1st edition, 01 2019.
- [7] C. J. M. Lasance. Ten years of boundary-condition-independent compact thermal modeling of electronic parts: A review. *Heat Transfer Engineering*, 29(2):149–168, 2008.
- [8] S. H. Anke, N. J. Ziegeler, P. W. Nolte, and S. Schweizer. Thermographic network identification for non-destructive testing. *16th Quantitative InfraRed Thermography Conference (QIRT)*, 2022.
- [9] M. Schmidt, S. K. Bhogaraju, A. Hanss, and G. Elger. A new noise-suppression algorithm for transient thermal analysis in semiconductors over pulse superposition. *IEEE Transactions on Instrumentation and Measurement*, 70:1–9, 2021.